URSI GASS 2020, Rome, Italy, 29 August - 5 September 2020

Indoor Measurement Based Verification of Ray Launching Algorithm at the Ka-Band

Wenfei Yang*(1)(3), Jie Huang(2), Jiliang Zhang(3), Sana Salous(2), and Jie Zhang(1)(3)
(1) Ranplan Wireless Network Design Ltd, Cambridge, U.K.
(2) Department of Engineering, Durham University, Durham, U.K.
(3) Department of Electronic and Electrical Engineering, The University of Sheffield, Sheffield, U.K.

Abstract

Ray launching (RL) algorithms are widely employed in indoor radio frequency (RF) design and planning, where a trade-off exists between the prediction accuracy and the computational cost. In this paper, a RL-based channel simulation is carried out in a simplified three-dimensional (3D) model of a typical classroom environment at the Ka-band. Channel measurements are conducted in a practical scenario to verify the accuracy of the simulations. The path loss and root mean square (RMS) delay spread of the propagation channel obtained from simulations and measurements are reported and compared, which show good agreements.

1 Introduction

The millimeter wave (mmWave) band with large unallocated sections of the spectrum is considered as one of the key solutions to extend the mobile capacity in indoor scenarios. However, the mmWave signals are vulnerable when propagating in a complex indoor environment due to various blockages [1, 2]. Therefore, it is critical to characterize the indoor channel accurately for indoor network deployment and optimization.

Conventionally, channel models are fitted from the measured data [3, 4, 5]. For complicated indoor environments, these empirical models show limited accuracy due to the lack of site-specific information. A more appropriate solution is to use ray-based deterministic models to characterise propagations in specific scenarios [6]. As one of the main types of ray-based models, ray launching (RL) algorithms are widely employed to simulate multipath propagations in indoor environments [7]. By discretizing the three-dimensional (3D) environment into unit sections, it can predict both time and spatial propagation parameters for the electromagnetic (EM) waves.

RL algorithms require the information of the propagation environment as input parameters, including the placement and specifications of the devices, the layout of the environment and EM properties of materials. Intuitively, the more detailed the environment is described, the higher the accuracy of the prediction. However, the large number of objects in the 3D space can result in difficulty in establishing the 3D environment model and a long computation time [8]. Additionally, the trade-off between the complexity and accuracy also exists when configuring the resolution of the environment discretisation [8], since the RL algorithm considers that the receivers in the same unit section receive the same multipath components. Therefore, balancing between the computational cost and the prediction accuracy is important when using RL algorithms in the design and planning of new wireless systems for buildings, especially in the mmWave band. The impact of simplification of the layout and the resolution of the environment discretization on the accuracy of the simulation can be evaluated through channel measurements.

In this paper, we present the validation of a RL-based channel simulation tool by channel measurements in a typical classroom scenario. A custom-designed frequency modulated continuous wave (FMCW) channel sounder at Durham University is used for channel measurements [9]. The simulation and measurements are conducted at 37–41.5 GHz (Ka-band) [10]. The power delay profiles (PDPs) are obtained from both the simulation and measurements for seventy data points in the scenario. The path loss and root mean square (RMS) delay spread are computed for each data point, and the overall validation results are analyzed.

2 Measurement and Simulation Parameters

2.1 The Propagation Environment

The simulations and measurements are carried out in a typical classroom scenario at Durham University, as shown in Fig. 1. It contains three rows of desks and chairs and other small objects such as a monitor and a projector. The room is rectangular with 8.6 m length, 7 m width and 2.8 m ceiling height. There are three sizable exterior glass windows which are 1.1 m above the floor and a door with the height of 2 m in this room. Outside the room is a long corridor connecting the other classrooms.

2.2 The RL-Based Simulation

A 3D model of the propagation environment is established for the RL-based simulation. As shown in Fig. 2, the main objects including the walls, floor, ceiling, windows, door

Figure 1. The classroom propagation scenario under measurement.

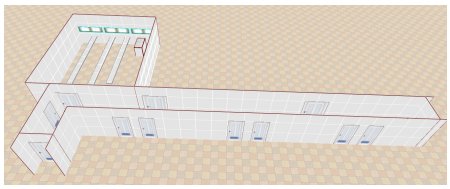

Figure 2. Simplified 3D model of the propagation environment for RL-based channel prediction.

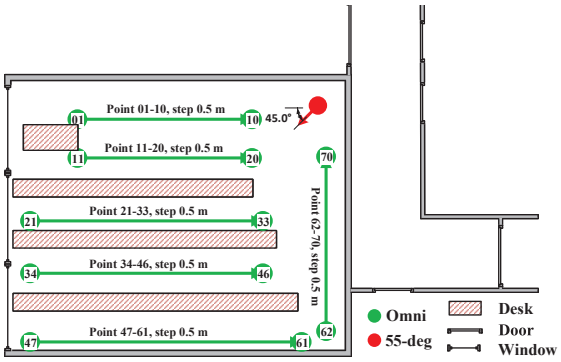

Figure 3. Plan of the propagation environment and the positions of the measurement points.

and desks are expressed in the model, while the other obstacles are omitted for simplification. The materials of the objects are configured according to the practical scenario prior to simulation.

The network system operating at the frequency band of 37-41.5 GHz is used in the simulation. The transmit antenna is a directional antenna with a $\sim$55° half-power beamwidth and the height is set 1.7 m above ground. The port power of the transmit antenna is set to 0 dBm. As shown in Fig. 3, the transmit antenna is located at the corner of the room and the main lobe pointed to the direction 45° in azimuth. The receive antenna is an omnidirectional antenna and fixed to 1.6 m high to mimic an average human height. A total of seventy locations of the user equipment (UEs) are considered and the positions are shown in Fig. 3.

The simulation is operated in a RL-based RF planning tool [11, 12, 13]. The resolution of the 3D propagation environment is 0.1 m. The simulation counted a maximum of five times of transmissions and five times of reflections for the rays. With these predefined simulation parameters, one single run of the simulation for this scenario takes around 2 minutes on a PC (Intel Core i7, 16 GB).

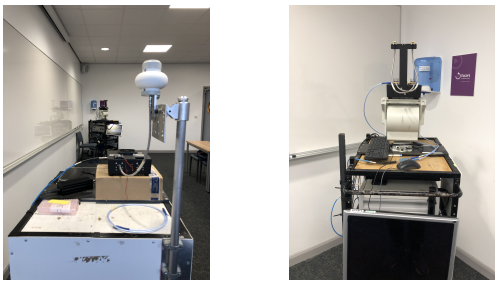

(a) Transmitter. (b) Receiver.

Figure 4. The mmWave channel sounder.

2.3 Channel Sounder and Measurement Parameters

In order to validate the simulation results, we carried out measurements in the descibed scenario. The transmitter and receiver are located on the positions marked by green and red dots in Fig. 3, respectively. During the measurements, the receiver location is fixed while the transmitter unit is moved onto the data points within the environment, imitating the positions of UEs in the simulation. The pictures of the receive and transmit antennas used in the measurements are shown in Fig. 4. The omnidirectional antenna with typical gain of $\sim$5 dBi is used at the transmitter. At the receiver, horn antenna with $\sim$10 dBi gain and the beamwidth on the order of $\sim$55° are used to match the device in the simulation. Both the transmit and receive antennas are vertically polarized. The received signal is compressed and down converted to baseband which is then sampled at a rate of 40 MHz. The waveform repetition frequency used in the measurements was 1.22 kHz.

3 Data Analysis and Results

3.1 The PDPs

The PDP for each data point is computed to compare the results in terms of time delay and power level of the multipath components. According to the propagation environment, a line-of-sight (LOS) component exists for each data point, which refers to the component arriving at the receiver without any obstruction. By aligning the time delay of the LOS component, the relative time delay and power level can then be compared between the measurement and the simulation.

Taking six data points in the environment as an example, the PDPs for these data points are shown in Fig. 5. For the first several arriving components, both the time delay and

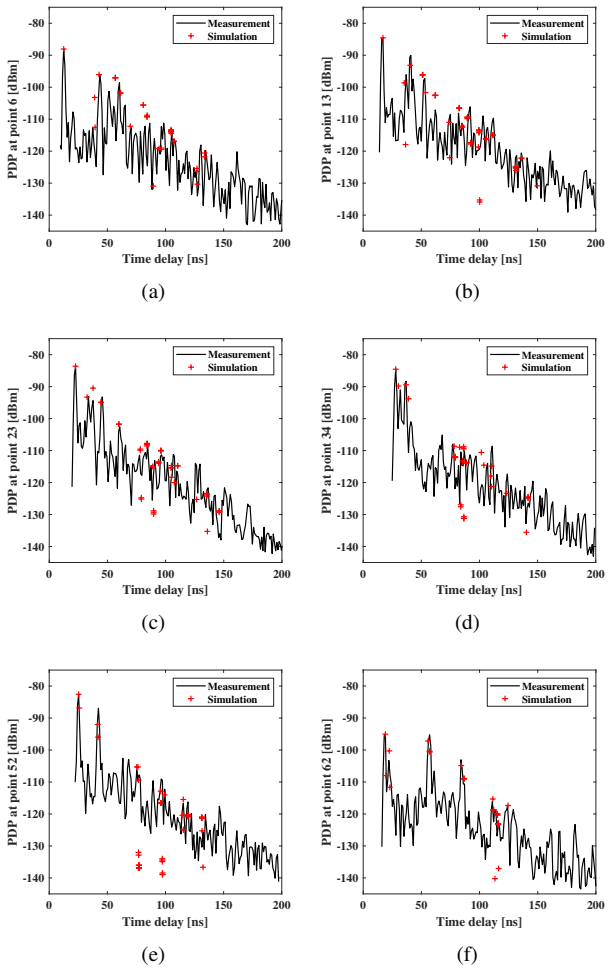

Figure 5. Comparisons between measurements and simulations of PDPs on measurement points in the classroom.

the power level of simulations, denoted by the red markers, fit the measured results well. For the other components with relatively low power, the trend of the simulation results shows good agreement with the measurements.

3.2 The RMS Delay Spread and Path Loss

The overall performance of the simulation is validated in terms of the time dispersive property and the path loss for each measurement point, which are the fundamental parameters considered for wireless system design.

The time dispersive properties of wideband multipath channels are commonly quantified by the RMS delay spread [3], which is the square root of the second central moment of the PDP and is defined by

$$\sigma = \sqrt{\frac{\sum_{k=1}^{K} P(\tau_k)\,\tau_k^2}{\sum_{k=1}^{K} P(\tau_k)} - (\bar{\tau})^2}, \tag{1}$$

where τ_k is the time delay for the k-th component arriving at the receiver relative to the first component and $P(\tau_k)$ is the

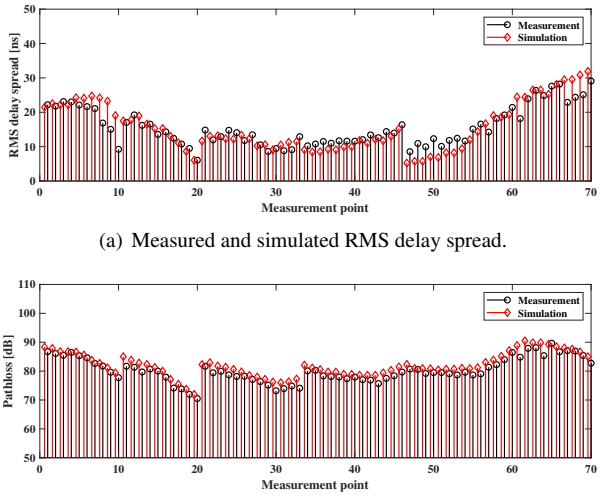

(a) Measured and simulated RMS delay spread.

(b) Measured and simulated path loss.

Figure 6. Comparison between measurements and simulations of the RMS delay spread and path loss for the measurement points in the classroom.

power of the k-th component. $\bar{\tau}$ denotes the mean excess delay and is computed by

$$\bar{\tau} = \frac{\sum_{k=1}^{K} P(\tau_k)\,\tau_k}{\sum_{k=1}^{K} P(\tau_k)}. \tag{2}$$

Path loss refers to the ratio between the transmitted power and received power excluding the overall system gain and antenna gains. As shown in Fig. 6, both the RMS delay spread and path loss obtained from the simulation results match the measurement results well.

3.3 Discussion

The validation results of both time dispersive properties and path loss of the channel show that the RL-based simulation can be considered as a reliable solution to predict the EM wave propagation in indoor scenarios for RF system design and planning at the Ka-band. Although the propagation environment has been simplified to save the time of computation, it shows a limited impact on the accuracy.

The difference between RL-based simulation and measurements could be attributed to the following: (1) Configurations of the propagation mechanisms in the simulation. The detection of transmissions and reflections of the rays are constrained within five times to reduce the computation time for each run of the simulation, which means that rays arriving at the receiver with more than five times transmission or reflections have been ignored in the simulation. In this rectangular room, the rays reflected more than five times are also recorded by the sounder but are not counted in the simulation. Therefore, taking -130 dBm as the threshold, the maximum excess delay for the simulation is shorter than the measurement, as shown in Fig. 5. (2) Environment

simplification. The 3D propagation environment model employed in the simulation is simplified from the exact scenario. The small objects, such as the monitor, projector and chairs, are not considered in the simulation. Therefore, multipath components reflected from these objects and received in the measurements could not be associated with the simulation results. (3) Configurations of the antennas and materials. Although the material database in the simulation is adjusted to match the practical scenario, error exists due to the complicated building construction materials. The radiation pattern of the antennas used in the simulation could also be mismatched due to side lobes.

Therefore, the accuracy of the simulations can be further improved by refining the simulation configurations including the layout of the propagation environment, the specifications of the devices and the EM properties of construction materials according to the measurement data. The calibrated database can be employed in the computation with a higher requirement of the accuracy and the longer time consumption tolerance.

In this paper, we focus on the propagation scenarios when there is a LOS path between the transmitter and the receiver. Another scenario that the transmitter and the receiver are separated by obstructions and thereby no LOS component exists is also commonly seen in the indoor environment. We leave the analysis of this scenario to future work. Moreover, the RL-based simulations will be validated in different propagation environments and also the influence of humans in the scenarios will be considered in future studies.

4 Conclusions

In this paper, we present a RL-based simulation of the EM wave propagation and the validation by measurements in a typical classroom environment in the Ka-band. Despite some simplifications of the propagation environment, the simulation results show good agreement with the measurements of different data points in terms of both path loss and time dispersive properties. Further studies will be carried out in the future to evaluate the prediction accuracy of the RL-based simulation in other scenarios.

Acknowledgement

The authors would like to acknowledge the support of EPSRC grant PATRICIAN EP/I00923X/1 under which the sounder was developed and the subsequent funding under Impact Acceleration Account (IAA) for the extension of the frequency range to the Ka-band. The authors would also like to thank Dr Y. Shao, Mr Y. Zhou, Mr S. Yang, Mr C. Chen and Mr Y. Yao for their contributions to the measurements and Dr Y. Gao and Dr J. Chen for their contributions to the data processing.

References

[1] T. S. Rappaport *et al.*, "Millimeter wave mobile communications for 5G cellular: It will work!," *IEEE Access*, vol. 1, pp. 335-349, 2013.

[2] J. Zhang *et al.*, "An experimental study on indoor massive 3D-MIMO channel at 30-40 GHz band," *International Symposium on Antennas and Propagation (ISAP)*, Busan, 2018, pp. 1-2.

[3] G. R. Maccartney *et al.*, "Indoor office wideband millimeter-wave propagation measurements and channel models at 28 and 73 GHz for ultra-dense 5G wireless networks," *IEEE Access*, vol. 3, pp. 2388-2424, 2015.

[4] S. Salous and Y. Gao, "Wideband measurements in indoor and outdoor environments in the 30 GHz and 60 GHz bands," *10th European Conference on Antennas and Propagation (EuCAP)*, Davos, 2016, pp. 1-3.

[5] 3GPP, "Studay on channel model for frequencies from 0.5 to 100 GHz," 3rd Generation Partnership Project (3GPP), *Tech. Rep.* TR 38.901 V14.1.1 Release 14, Aug. 2017. [Online]. Available: http://www.3gpp.org/DynaReport/38901.htm

[6] Z. Yun and M. F. Iskander, "Ray tracing for radio propagation modeling: Principles and applications," *IEEE Access*, vol. 3, pp. 1089-1100, 2015.

[7] Q. Hong *et al.*, "The impact of antenna height on 3D channel: A ray launching based analysis," *Electronics*, vol. 7, no. 2, Jan. 2018.

[8] J. S. Lu *et al.*, "A discrete environment-driven GPU-based ray launching algorithm," *IEEE Trans. Antennas Propag.*, vol. 67, no. 2, pp. 1180-1192, Feb. 2019.

[9] S. Salous *et al.*, "Wideband MIMO channel sounder for radio measurements in the 60 GHz band," *IEEE Trans. Wireless Commun.* , vol. 15, no. 4, pp. 2825-2832, Apr. 2016.

[10] Resolution 238. *In Proceedings of the World Radio Communications Conference*, Geneva, Switzerland, Nov. 2015.

[11] Ranplan Professional. [Online]. Available: https://ranplanwireless.com

[12] Z. Lai *et al.*, "On the use of an intelligent ray launching for indoor scenarios," *4th European Conference on Antennas and Propagation (EUCAP)*, Barcelona, 2010, pp. 1-5.

[13] Z. Lai *et al.*, "Implementation and validation of a 2.5D intelligent ray launching algorithm for large urban scenarios," *6th European Conference on Antennas and Propagation (EUCAP)*, Prague, 2012, pp. 2396-2400.